Dendrites enable a robust mechanism for neuronal stimulus selectivity

Romain D. Cazé[1,*], Sarah Jarvis [1], Amanda J. Foust[1], Simon R. Schultz[1],

1 Centre for Neurotechnology and Department of Bioengineering, Imperial College London, South Kensington, London, SW7 2AZ, UK

*** romain.caze@gmail.com**
Keywords: Dendrites — stimulus selectivity — single neuron computation

Abstract

Hearing, vision, touch – underlying all of these senses is stimulus selectivity, a robust information processing operation in which cortical neurons respond more to some stimuli than to others. Previous models assume that these neurons receive the highest weighted input from an ensemble encoding the preferred stimulus, but dendrites enable other possibilities. Non-linear dendritic processing can produce stimulus selectivity based on the spatial distribution of synapses, even if the total preferred stimulus weight does not exceed that of non-preferred stimuli. Using a multi-subunit non-linear model, we demonstrate that selectivity can arise from the spatial distribution of synapses. Moreover, we show that this implementation of stimulus selectivity increases the neuron's robustness to synaptic and dendritic failure. Contrary to an equivalent linear model, our model can maintain stimulus selectivity even when 50% of synapses fail or when more than 50% of dendrites fail. We then use a Layer 2/3 biophysical neuron model to show that our implementation is consistent with recent experimental observations, of a mixture of selectivities in dendrites, that can differ from the somatic selectivity, and of hyperpolarization broadening somatic tuning without affecting dendritic tuning. Our model predicts that an initially non-selective neuron can become selective when depolarized. In addition to motivating new experiments, the model's increased robustness to synapses and dendrites loss provides a starting point for fault-resistant neuromorphic chip development.

Author summary

From the stripes of your shirt to the sound of your grandmother's name, your neurons are capable of selecting among stimuli. How do they perform this selection? The standard model assumes that a neuron receives the strongest inputs from neurons encoding its preferred stimulus. While this can explain many observations, it neglects dendrites, the neuron's "antennae" for receiving inputs. Here we propose an alternate non-linear model for stimulus selectivity which incorporates dendrites fitting with the latest experimental observations and more robust than a linear model all other things being equal. This additional robustness enabled by dendrites offer new possibilities for neuromorphic chip design.

1 Introduction

Over 50 years ago, Hubel and Wiesel discovered an example of neuronal stimulus selectivity [1], in which certain neurons in the visual cortex respond maximally to particular visual stimuli. They proposed a single compartment model integrating its input linearly to account for this selectivity. This model however neglects dendrites.

Several groups have recently presented data which is counter-intuitive given the Hubel and Wiesel model. Firstly, this model integrates inputs with a narrow range of selectivity. In contrast, some experimental groups observed a mixture of selectivity [2,3]. Specifically, Smith et al performed dual soma-dendrites recordings and they have demonstrated that somatic and dendritic tuning could differ [4]. Moreover, Jia and colleagues have shown using calcium imaging that the tuning of dendritic hotspots could also differ from the somatic tuning [3]. Secondly, it was observed that hyperpolarization can significantly broaden somatic tuning, while dendritic tuning stays sharp [3]. The first set of observations can be explained in a Hubel and Wiesel type model by using a higher number of synapses for preferred than non-preferred stimuli. It is more difficult however to explain the second set of observations with a Hubel and Wiesel model. Why hyperpolarization does not also broaden dendritic tuning like it does for somatic tuning? Taken together these two sets of observations call for models more complex than a single linear compartment and in this paper we propose that they can be accounted for by the properties of dendrites.

Biophysical studies from the 80s and 90s demonstrated that a neuron can be sensitive to the spatial distribution of synaptic inputs because of its dendrites [5,6]. Mel and colleagues have shown that a neuron could respond more intensely to clustered than dispersed inputs [5,7]. Alternatively, Koch and colleagues have had demonstrated that under other conditions the opposite can also be true: a neuron can respond more to dispersed than clustered inputs [6]. Our previous studies built on these biophysical findings and demonstrated that dendrites extend the computational capacity of a single neuron [8,9]. Recent experimental evidence has shown that excitatory synapses distribute non-randomly on dendrites and can form synaptic clusters [10–12]. We examine here whether we can employ the spatial distribution of excitatory synapses to implement stimulus selectivity. We show that such an implementation is more robust than a linear equivalent model and propose that it could better explain the recent experimental data.

2 Results

Dendrites allow stimulus selectivity based on the spatial distribution of synapses

We began by using a multi-subunit model sensitive to the spatial distribution of synapses. Each subunit processes its input independently with the same non-linear transfer function (Fig. 1A) to account for the non-linear integration observed in dendrites [13–16]. A subunit could be seen as a primary dendrite emerging from a multipolar neuron. A cluster of active synapses on a subunit generate a single dendritic spike whereas a dispersed synaptic activity on multiple subunits can generate more spikes. In this model, as *in vivo* [17,18], the generation of an action potential requires multiple dendritic spikes; in our model, at least 20 % of subunits need to emit a dendritic spike to trigger an action potential. Because of this property, our model will be more likely to fire an action potential when synaptic activation is distributed across multiple subunits rather than clustered onto a single subunit.

We use this sensitivity to generate stimulus selectivity in our model. Table 1 depicts

the mean number of synapses per subunit depending on the ensemble of origin. We grouped input neurons in eight different ensembles and each ensemble activates synchronously depending on the stimulus. On the one hand, the ensemble encoding the preferred stimulus distribute its 750 synapses randomly following a uniform law. On the other hand, ensembles encoding the non-preferred stimuli cluster 40% of their 600 synapses on a given subunit and distribute the remaining synapses following a uniform law on all the other subunits. We present an instance of this distinction in Fig. 1B. Fig. 1C-D shows how the eight distinct ensembles distribute their synapses (Red:Preferred, Black/Grey:Non preferred) on our our multi-subunit and our biophysical stimulus selective neuron model.

Two recent papers describe how such a spatial distribution of synapses could be learned [19, 20]. Please note that we also proposed a learning algorithm presented in a self-archived manuscript currently under review [21].

Spatial distribution based stimulus selectivity increases robustness to synaptic and dendritic failure

In this section, we probe the robustness of our implementation by comparing two equivalent multi-subunit models in which integration is either linear or non-linear. 10 % of synaptic activity triggers a dendritic spike in a subunit of the non-linear model, whereas a subunit in the linear model never spikes, and never saturates.

In a linear model it is necessary that the preferred ensemble makes the strongest contact, i.e. makes the highest number of synaptic contacts. A linear model stops being selective for the previously preferred stimulus when a non-preferred stimulus makes stronger contacts than the preferred stimulus (Fig. 2A, black), for which proof is given in Methods. The non-preferred stimulus making the highest number of contacts then becomes the preferred stimulus. Conversely, our non-linear model remains stimulus selective even when the preferred stimulus ensemble forms 200 fewer synapses than non-preferred stimulus ensembles (Fig. 2A, red). This property of our non-linear model confers robustness against synaptic failure (Fig. 2B), where a synapse stays inactive when it should be active. It can separate both types of stimulus (Fig. 2C) and can maintain its function after 50% of its synapses fail (Fig. 2D). In conclusion, for an equivalent number of synapses a multi-subunit non-linear is more robust than its linear counterpart.

A non-linear model also maintains its function when dendrites are disabled. This could occur when a dendrite is physically pruned from the neuron. Our multi-subunit non-linear model maintain its function even if only 25% of its synapses cluster on a single subunit as shown in Fig. 3A (red). This considerably boosts the stability of the non-linear model, which can maintain functionality even under the loss of more than 50% of compartments (Fig. 3B, black and Fig. 3C). In comparison, a linear model cannot use the spatial distribution of synapses and if the synaptic bias is nil, it is impossible to differentiate preferred and non-preferred stimuli (Fig. 3A, black). The clustering bias (here 30 %) is detrimental for this type of model. It makes the linear model sensitive to the loss of even a single compartment (Fig. 3B black). Fig. 3D shows that it is impossible for a linear model losing four dendrites to separate the preferred and non-preferred stimuli.

In summary, we compared two multi-subunit models: a linear and a non-linear model. We used simulations to demonstrate that the non-linear model is much more robust than its linear equivalent. We have shown that non-linear dendrites offer a new dimension of robustness. Our non-linear multi-subunit model can lose 50% (more than 2600) of its synapses or more than 50% of its dendrites (more than 4) while maintaining its function.

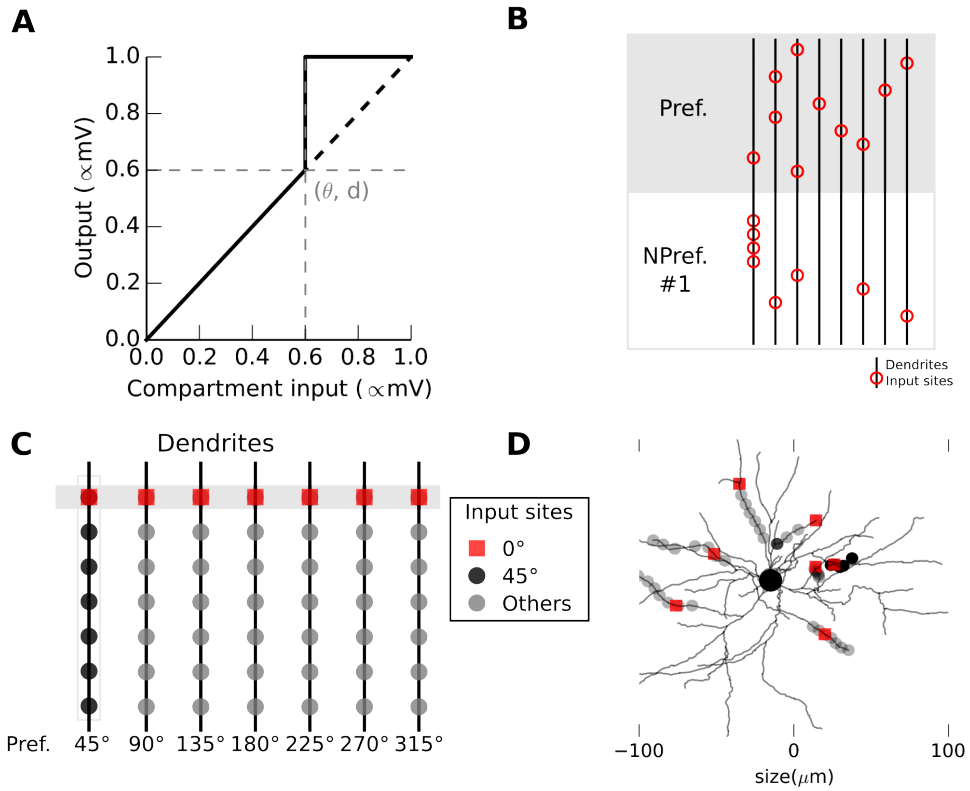

Figure 1. Non-linearities enable stimulus selectivity using the spatial distribution of synapses. (A) Local transfer function within a subunit; a non-linear jump occurs at the point (θ, d). Input and output are normalized given their respective maxima. (B) The input sites (red circles) on dendrites (horizontal lines) are where the highest number of synaptic contacts are made (at most 70 synapses). The preferred stimulus (Pref.) makes the highest number of synapses and the most scattered distribution. (C-D) Schematic depiction of the spatial distribution of synapses on dendrites (red: preferred 0, black/gray: non-preferred from 45 to 315). (C) Because of the following synaptic placement (circles and squares) each subunit (vertical lines) displays a distinct selectivity. Pref (shaded area) and NPref are respectively scattered or clustered. (D) Localization of the input sites on a stimulus selective biophysical model of a L2/3 neuron.

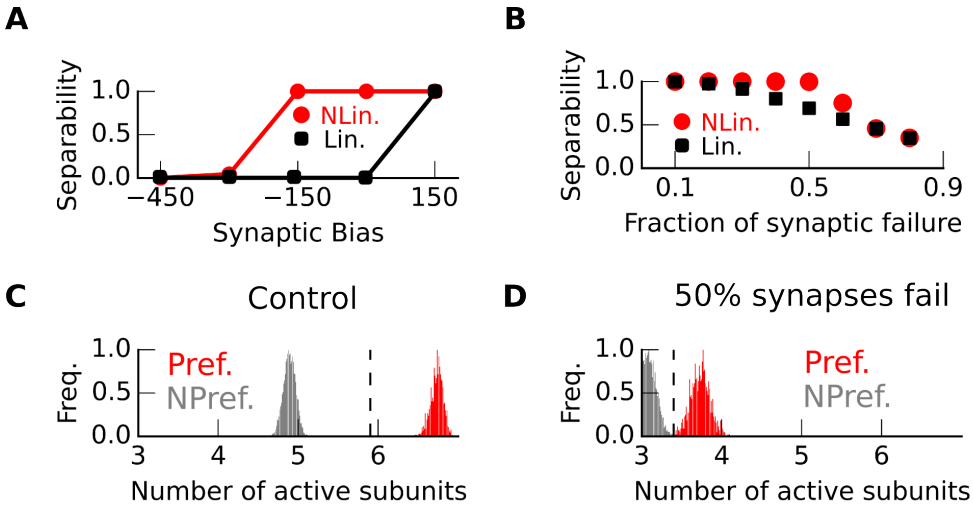

Figure 2. Stimulus selectivity achieved with the spatial distribution of synapses increases the robustness to synaptic failure. (A-B) Separability, calculated as the fraction of model capable of separating preferred and non-preferred stimuli (over 1000 model following the synaptic distribution depicted in Table 1), for the non-linear (red circles) and linear (black square) models as a function of (A) the synaptic bias, which is the difference in the number of synapses between preferred and non-preferred ensemble; or (B) the synaptic failure which is the fraction of malfunctioning synapses. (C-D) Number of spiking/active subunits in a model with seven subunits. Distribution for preferred (red) and non-preferred stimuli (gray) (C) In control condition, or (D) with 50% synapses failing.

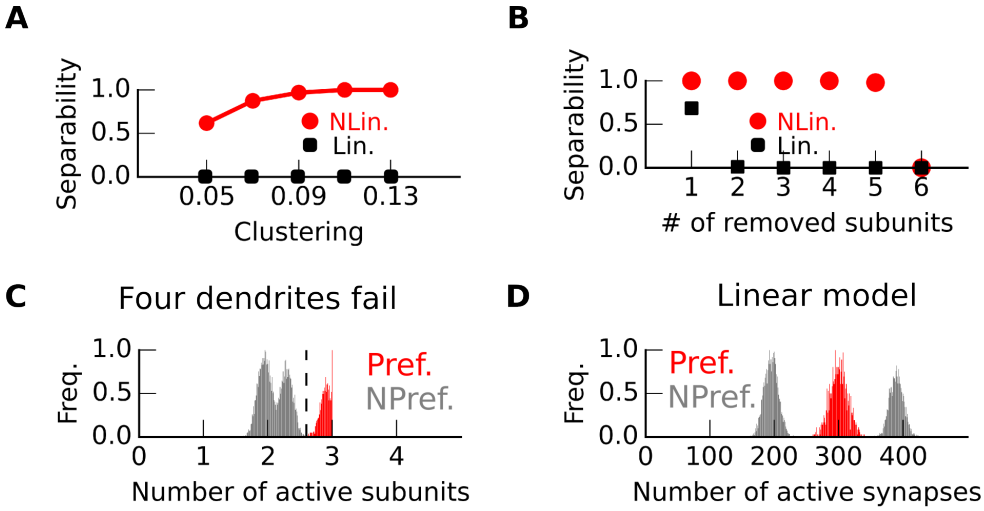

Figure 3. Stimulus selectivity achieved with spatial distribution of synapses increases the robustness to dendritic failure. (A-B) Separability, calculated as the fraction of models capable of separating preferred and non-preferred stimuli ($n = 1000$), for the non-linear (red circles) and linear (black square) model as a function of (A) the clustering bias, which is the number of synapses specifically set on a precise compartment; and (B) the number of removed compartments. (C-D) Distribution of dendritic activity for preferred (red) and non-preferred (gray) (C) in the non-linear models where dendritic activity closely relates to the number of maximally active compartment; and (D) in the linear model, where synaptic activity is the number of active synapses.

The biophysical model replicates the mixture of dendritic tunings

We have shown how a multi-subunit non-linear model can robustly implement stimulus selectivity. The following section demonstrates that these results carry over to a biophysical model capturing rich temporal dynamics and interactions between compartments. This biophysical model fits recent experimental observations [3].

We constructed a stimulus selective neuron (Fig. 4A) that replicates the experimental data. Both the data and our model can display a variety of dendritic tunings (Fig. 4B-C). To replicate the experimental observations, we used 8 ensembles of AMPA/NMDA-type synapses distributed each on 7 locations. Synapses from the preferred stimulus ensemble scatter across all branches, whereas synapses from the non-preferred ensembles cluster, each onto a particular dendrite. We placed these synapse on a Layer 2/3 neuron reconstruction [3] (Fig. 1D).

The activation of a synapse results in a somatic depolarization of $\frac{1}{7}$ mV, independent of its location (Fig. 4C), as has been observed in another cell type [4]. We enforced this "dendritic democracy" [22] by scaling synaptic conductances depending on their distance to the soma. Consequently, all synapses produce the same depolarization at the soma and each ensemble makes the same number of synapses. Therefore, in theory all ensemble should produce the same depolarization at the soma, but this is not exactly the case in practice because of non-linear interaction between synapses.

Interestingly, synapses interact in two distinct ways, dependent on their location. For synapses clustered on a branch (Fig.1D black squares and Fig. 4C, black trace), seven active synapses (one per location, Fig.1D presents the 8 sets of 7 locations) interact supra-linearly and they produce a depolarization superior to one mV because they generates an NMDA spike [23], but 35 synapses on a branch (five per location) interact sub-linearly due to reduced driving force at synapses [6, 24]. Even if the depolarization at the soma is weak, locally, the membrane voltage within a branch reaches the equilibrium voltage (0 mV) because of the branch small diameter 1 μm (see Movie S1). In contrast, for synapses scattered across the seven branches, scattered stimulation depolarizes the soma more than clustered synapses because multiple NMDA spikes are generated (Fig. 4C, red trace) as has been observed experimentally *in vivo* [17]. These observations are summarized in an expected/measured plot (Fig. 4D) and show the biophysical model's sensitivity to the synaptic spatial distribution.

This sensitivity enables the generation of stimulus selectivity in our model. If the population coding for the preferred stimulus makes functional synapses on all primary dendrites, whereas non-preferred stimuli cluster on single branches, then the distributed synaptic arrangement produces multiple NMDA spikes that reach the soma in parallel, as observed *in vitro* [25] and *in vivo* [18, 26] (Fig. 4A). Both scenarios are illustrated in animations provided as supplementary material (see movies S1 and S2).

In a single compartment model, the highest weighted stimulus always "wins", rendering synaptic spatial distribution irrelevant. Conversely, our multi-compartment biophysical model uses exclusively the spatial distribution of synapses to implement stimulus selectivity, a configuration that could explain, in contrast with single compartment models, how calcium hotspots in dendrites display mixed stimulus tuning [3]. Note that our model does not exclude an average dendritic tuning similar to the somatic tuning, however it can explain the cases where the average dendritic tuning differs from somatic tuning.

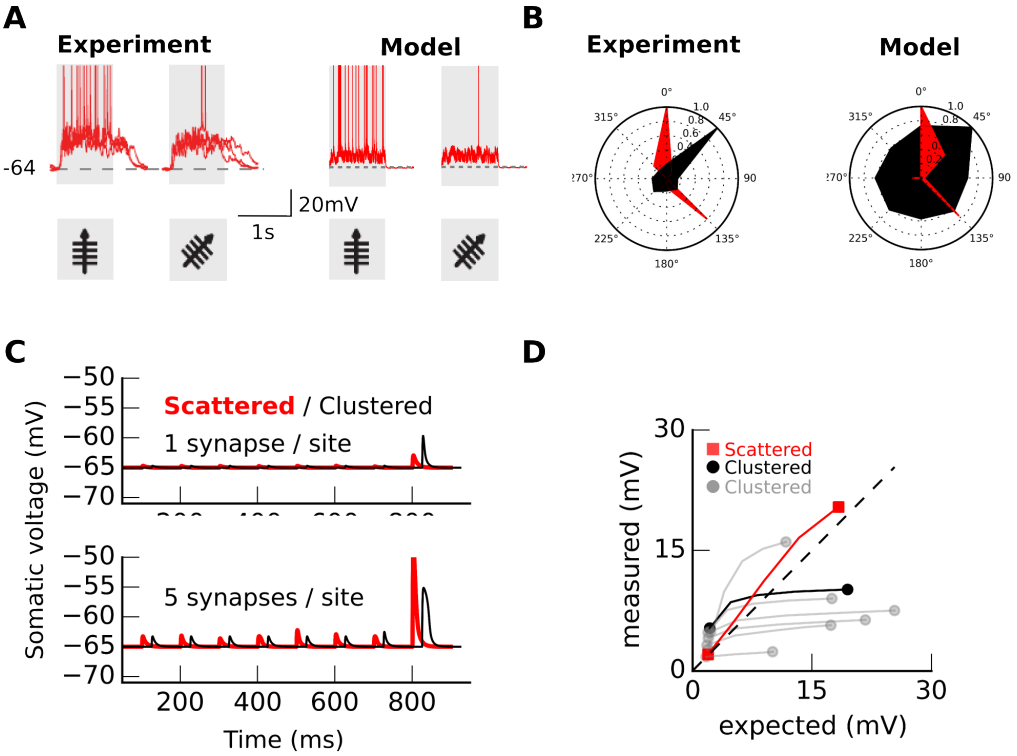

Figure 4. Stimulus selectivity implemented through the spatial distribution of synapses displays a mixture of dendritic selectivities. (A) Somatic voltage for two stimuli (0/45 degrees during shaded period). (B) Spike count (red) and selectivity in dendrites (one example; black, calcium signal integral in the experiment and integral of the membrane voltage in the model). (C) Somatic depolarization when one(top)/five(bottom) synapse(s) activate in one of the input sites from 0 to 800 ms; or when one/five occurs at all the 7 sites (800 to 1000ms). Input locations are described in Fig. 1 (red: scattered/black: clustered). (D). Expected (arithmetic sum) versus measured depolarization in the 8 sets (red:scattered on 7 branches, black/grey:clustered on a branch) of 7 input sites. Black and red marks correspond to experiments carried out in (C)

Hyperpolarization broadens somatic but sharpens dendritic tuning in our model

We injected current at the soma in our biophysical model to pull down the membrane potential from -65mV to -70mV, as in Jia et al.'s experiment [3]. Because of hyperpolarization, the neuron stops firing action potentials, and the somatic tuning of the membrane voltage becomes broader. This might be mainly due to the non-linearity induced by somatic spiking in the control condition. The dendritic tuning, however, is sharp even under hyperpolarization.

When we decrease the resting membrane voltage to -70mV, the number of synapses necessary to trigger an NMDA spike increases, and only the dendritic preferred stimulus provokes an NMDA spike. Fig. 5A shows that only the 45 degree stimulus triggers dendritic spikes, and dendritic selectivity sharpens (Fig. 5B). Conversely, the somatic depolarization difference between scattered and clustered synapses decreases, when we hyperpolarize the neuron (Fig. 5C-D), and somatic selectivity broadens.

The model's sensitivity to the spatial distribution of synapses predicts the effect of hyperpolarization on dendritic tuning. The broadening of the somatic tuning can intuitively be explained by hyperpolarization. Intuitively, somatic spiking non-linearly sharpens somatic tuning in the control condition. The sharp dendritic tuning however is much less intuitive, and the sharpening of dendritic tuning during hyperpolarization is another important prediction of our modeling work. This could be tested by using micro-injection of TTX, or a similar approach, instead of hyperpolarization to block back-propagated action potentials.

3 Discussion

We implemented stimulus selectivity in a multi-subunit non-linear model (Fig. 1) that can lose 50% synapses or more than 50% of its subunits and maintain its function (Fig. 2). Importantly, the selectivity mechanism we propose can coexist with a classical mechanism based upon synaptic strength (Fig. 4A), providing an additional channel for neuronal information processing. In practice, the ensemble encoding the preferred stimulus does make the strongest contact, as suggested by Cossel et al [27] and observed by Chen et al [28]. A linear model can also be robust if there is a large difference in the number of synapses between preferred and non-preferred ensembles. In our study, we used the same synaptic difference in the non-linear and the linear model to show that using the spatial distribution of synapses adds a new dimension to robustness. Although the two models detailed in the manuscript exhibit average dendritic tuning different to that of the soma, these models also allow for the possibility that the average dendritic tuning is similar to the somatic tuning.

Local and non-linear integration could have made our model cluster sensitive. Instead it responds more to scattered (widely distributed) synaptic activity. This behavior has previously been described [5, 6], but has never been proposed as a mechanism underlying stimulus selectivity. Recent unexpected experimental observations [3] motivated our use of scatter sensitivity, rather than cluster sensitivity, for this purpose. Additional experimental work, for instance where dendrites are disabled using targeted laser dendrotomy, will however be necessary to confirm the functional role of scatter sensitivity [29]. This work could test our first prediction, that stimulus selectivity is stable to dendrites removal. Futhermore, functional connectomics will enable us to determine experimentally whether clustered and scattered synapses encode non-preferred and preferred stimuli.

Although we have focused, to ease comparison with experimental studies, on the tuning of a neuron to a sensory stimuli, all neural computations can be described in

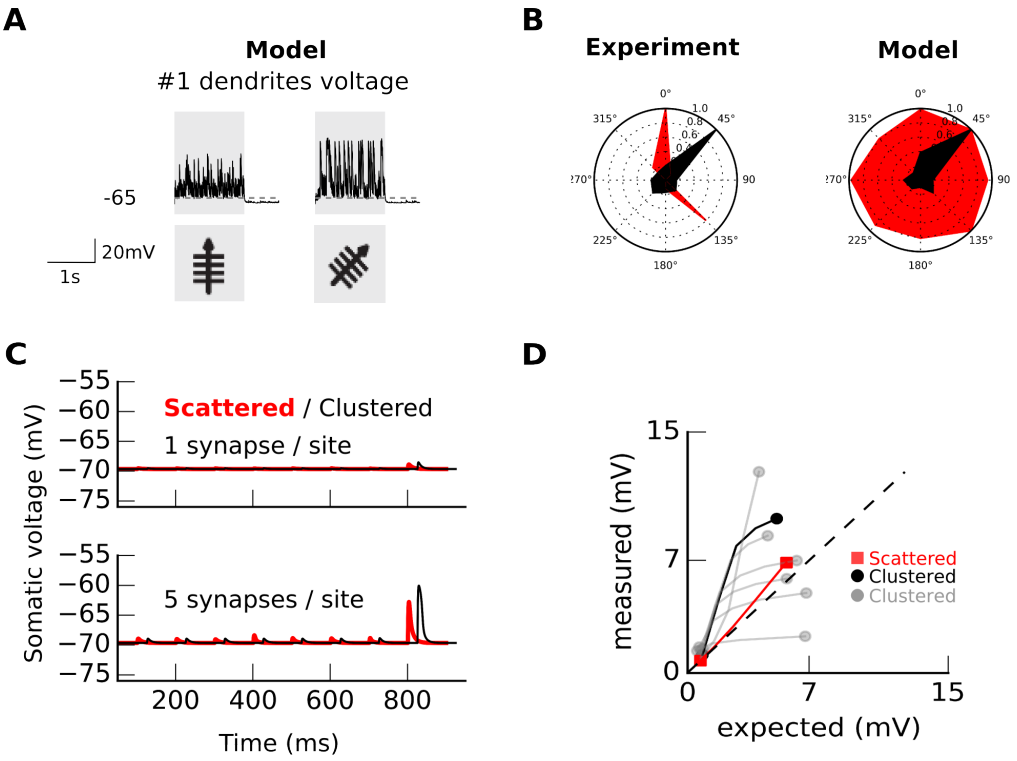

Figure 5. Hyperpolarization broadens somatic tuning whereas it sharpens dendritic tuning in our model. (A) Local membrane potential in the first dendritic branch for two stimuli: the soma's preferred stimulus and for the dendrite's preferred stimulus. (B) Integral of dendritic calcium signal (black) and of the somatic membrane voltage (red) (replotted from [3]). In our model we compute the integral of the dendritic membrane voltage (black). (C) Somatic depolarization when one(top)/five(bottom) synapse activate in one of the input site from 0 to 800 ms; or when one/five occurs at all the 7 sites (800 to 1000ms). Input locations are described in Fig. 1 (red: scattered/black: clustered). (D). Expected (arithmetic sum) versus measured depolarization in the simulation 2 sets of 7 locations.

terms of stimulus selectivity. Boolean functions can both describe a neural computation and stimulus selectivity. In the latter case, we can describe stimuli as words of 0s and 1s. In the former case, we can describe all neural computations as Boolean functions if we binarize activity. Therefore our implementation based on the spatial distribution of synapses can be used for general neural computation. To transpose a synaptic strength based implementation of a computation, it suffices to turn the strength of a weight into a dispersion factor.

The biophysical model reinforces our claim that the insights gained from the multi-subunit model are physiologically relevant; together, they yield three predictions. Firstly, we predict that hyperpolarization not only broadens somatic tuning [3, 30] but it also sharpens dendritic tuning (Fig. 5). Our results, taken together, make two testable predictions. Secondly, our model predicts that a neuron may recover its tuning after losing a large fraction of either its synapses or dendrites, due to the robustness provided by spatial synaptic distribution based information processing. Thirdly, we predict that a cortical neuron with no apparent stimulus tuning can acquire stimulus selectivity when depolarized, similar to what can be observed in place cells [31].

Our implementation using nonlinear dendritic integration may inform the design of neuromorphic chips, as it suggests that the use of dendrites – even passive – can extend the robustness of the circuit. Dendrites may not only increase the computational power of each unit [8], but also increase their resilience, addressing a crucial issue in the design of fault-tolerant chip architectures. While we have demonstrated these capabilities in the context of a neuron's selectivity to a visual stimulus, the model we have proposed is general, and potentially reflects a canonical computational principle for neuronal information processing.

4 Methods

Multi-subunit model

Our multi-subunit model consists of seven subunits, each receiving input from eight presynaptic neuronal ensembles corresponding to eight different stimulus orientations. The mean number of synaptic contacts for each ensemble-dendrite pair is described in Table 1. The preferred stimulus (0 degrees) activates 700 synapses following a random uniform distribution across all seven dendrites. In contrast, non-preferred stimuli activate 650 connections each, including a bias such that 40% of input from each orientation preferentially target one of the dendrites and the remaining 60% being uniformly distributed among the remaining six dendrites following a uniform distribution. A dendrite saturates when 100 of its synapses are active, and the somatic output will be determined by the arithmetic sum of all the dendritic output.

A necessary condition for the linear model

The highest weight needs to be from the preferred stimulus in a linear model. To prove that let us consider the simplest scenario where two presynaptic neurons each synapse onto a postsynaptic neuron. We arrange it so that one input codes for the preferred stimulus while the other for a non-preferred stimulus, and W_{pref} and W_{nonpref} is the amplitude of their resulting depolarization on the postsynaptic neuron. Here, stimulus selectivity is possible only if $W_{\text{pref}} \geq \Theta$ and $W_{\text{nonpref}} < \Theta$, which is equivalent to $W_{pref} > \Theta > W_{\text{nonpref}}$. This condition can be generalized for any number of presynaptic neurons, and implies in the linear neuron model when constrained to positive values of W that stimulus selectivity is only possible when the preferred stimulus has the highest weight.

Table 1. Synaptic distribution in our multi-subunit model. Mean number of synapses made by each presynaptic ensemble for each stimulus, for each postsynaptic dendrite.

	Dendrite (d_j)							
Preferred orientation	0	1	2	3	4	5	6	Total
0	100	100	100	100	100	100	100	700
45	260	65	65	65	65	65	65	650
90	65	260	65	65	65	65	65	650
135	65	65	260	65	65	65	65	650
180	65	65	65	260	65	65	65	650
225	65	65	65	65	260	65	65	650
270	65	65	65	65	65	260	65	650
315	65	65	65	65	65	65	260	650

Biophysical model

For detailed modeling, we used a reconstructed morphology of a neuron from Layer 2/3 of visual cortex in mouse [3]. The capacitance of the model is $C = 1\mu F/cm^2$. The axial resistance in each section was $R_a = 35.4\Omega$, and passive elements were included ($g_l = 0.001\ \Omega^{-1}$, $e_l = -65$ mV). To hyperpolarize the neuron to $-70mV$ we injected $0.15nA$ which gives an input resistance of $33.3M\Omega$. Spiking was implemented using an integrate-and fire mechanism with a hard threshold of -45mV, which has been shown to provide an accurate depiction of spike initiation behaviour [32], whereupon we set the voltage to 20 mV in the following timestep, before resetting to -65 mV. The model was implemented using NEURON with a Python wrapper [33], with the time resolution set to 0.1ms.

Synaptic inputs to the biophysical model

We used 280 synapses divided into 8 groups of 35 synapses, corresponding to 8 different stimuli (orientations). Each had a background activity of 1 Hz which increased to 10Hz during the presentation of the stimulus. As experimental evidence suggests that stimulus information is coded not only by an increase in firing rate but also in correlation [34, 35], synapses synchronously co-activate 20 times to encode the presence of a stimulus (preferred or otherwise). This raises the firing rate of this group to 30 Hz. The specific set of synchronous synapses activated depends on the stimulus identity, e.g. synapses 1-35 synchronously activate for the preferred stimulus, synapses 36-70 activate for the non-preferred stimulus #1, etc.

Conductance based NMDA-type synapses

NMDA-like inputs were included by modeling voltage-dependent, conductance-based synapses that generated postsynaptic currents $i_s = g(t)g_{\mathrm{mg}}(v) \times (v(t) - e_s)$, with reversal potential e_s =0 mV. For $g(t)$, we used an alpha-function with rise and decay time constants $\tau_1 = 0.1$ms and $\tau_2 = 10$ms respectively. Values for τ_1 and τ_2 were chosen to be deliberately lower than those for real glutamate binding on NMDA channels to account for the presence of voltage-gated calcium dependent potassium channels in the membrane. The voltage-dependent conductance $g_{mg}(v)$ was determined assuming $[\mathrm{Mg}^{2+}]$ =1mM. The equation for the Mg block was $g_{Mg}(v) = \frac{1}{1-ve^{0.062}} \times \frac{1}{3.57}$.

Supporting Information

S1 Video

Neuron response to clustered synaptic inputs. L2/3 neuron reconstruction from the visual cortex. The large circle is the soma and black dots are input sites. Depolarization of a section is color-coded (black:low, yellow:high).

S2 Video

Neuron response to scattered synaptic inputs. L2/3 neuron reconstruction from the visual cortex. The large circle is the soma and black dots are input sites. Depolarization of a section is color-coded (black:low, yellow:high).

Acknowledgments

The authors thank Dr Hongbo Jia for providing the Layer 2/3 neuron reconstruction used for the model presented in this paper, and Dr. Andrew Gallimore, Dr. Mark Humphries, Dr. Boris Gutkin, Dr. Fleur Zeldenrust and Dr Matthijs Van Der Meer for their comments on the draft manuscript. This work was supported by EU FP7 Marie Curie Initial Training Network 289146. SJ is supported by EU FP7 Marie Curie fellowship (PIEF-GA-2013-628086), and SRS by a Royal Society Industry Fellowship.

References

1. Hubel DH, Wiesel TN. Receptive fields of single neurones in the cat's striate cortex. The Journal of Physiology. 1959;148:574–591.

2. Smith SL, Smith IT, Branco T, Häusser M. Dendritic spikes enhance stimulus selectivity in cortical neurons in vivo. Nature. 2013 oct;503(7474):115–20. Available from: `http://www.ncbi.nlm.nih.gov/pubmed/24162850`.

3. Jia H, Rochefort NL, Chen X, Konnerth A. Dendritic organization of sensory input to cortical neurons in vivo. Nature. 2010;464(7293):1307–1312. Available from: `http://www.nature.com/doifinder/10.1038/nature08947`.

4. Smith MA, Ellis-Davies GCR, Magee JC. Mechanism of the distance-dependent scaling of Schaffer collateral synapses in rat CA1 pyramidal neurons. The Journal of Physiology. 2003;548(1):245. Available from: `http://www.jphysiol.org/cgi/doi/10.1113/jphysiol.2002.036376http://jp.physoc.org/content/548/1/245.short`.

5. Mel BW. Synaptic integration in an excitable dendritic tree. Journal of Neurophysiology. 1993 sep;70(3):1086–101. Available from: `http://www.ncbi.nlm.nih.gov/pubmed/8229160`.

6. Koch C, Poggio T, Torres V. Retinal ganglion cells: a functional interpretation of dendritic morphology. Phil Trans R So Lond B. 1982;298(1090):227–263. Available from: `http://rstb.royalsocietypublishing.org/content/298/1090/227.short$\delimiter"026E30F$nhttp://rstb.royalsocietypublishing.org/cgi/doi/10.1098/rstb.1982.0084`.

7. Poirazi P, Brannon T, Mel BW. Pyramidal neuron as two-layer neural network. Neuron. 2003 mar;37(6):989–999. Available from: http://www.ncbi.nlm.nih.gov/pubmed/12670427http://www.sciencedirect.com/science/article/pii/S0896627303001491.

8. Cazé RD, Humphries M, Gutkin BS. Spiking and saturating dendrites differentially expand single neuron computation capacity. Advances in neural information processing systems. 2012;25:1–9. Available from: http://books.nips.cc/papers/files/nips25/NIPS2012{_}0519.pdf.

9. Cazé RD, Humphries M, Gutkin B. Passive Dendrites Enable Single Neurons to Compute Linearly Non-separable Functions. PLoS Computational Biology. 2013;9(2).

10. Takahashi N, Kitamura K, Matsuo N, Mayford M, Kano M, Matsuki N, et al. Locally Synchronized Synaptic Inputs. Science. 2012 jan;335(6066):353–356. Available from: http://www.sciencemag.org/cgi/doi/10.1126/science.1210362.

11. Druckmann S, Feng L, Lee B, Yook C, Zhao T, Magee JC, et al. Structured Synaptic Connectivity between Hippocampal Regions. Neuron. 2014;81(3):629–640. Available from: http://dx.doi.org/10.1016/j.neuron.2013.11.026.

12. Kleindienst T, Winnubst J, Roth-Alpermann C, Bonhoeffer T, Lohmann C. Activity-Dependent Clustering of Functional Synaptic Inputs on Developing Hippocampal Dendrites. Neuron. 2011 dec;72(6):1012–1024. Available from: http://linkinghub.elsevier.com/retrieve/pii/S0896627311009263.

13. Polsky A, Mel BW, Schiller J. Computational subunits in thin dendrites of pyramidal cells. Nature Neuroscience. 2004 jun;7(6):621–627. Available from: http://www.ncbi.nlm.nih.gov/pubmed/15156147.

14. Tamás G, Szabadics J, Somogyi P. Cell type- and subcellular position-dependent summation of unitary postsynaptic potentials in neocortical neurons. Journal of Neuroscience. 2002 feb;22(3):740–747. Available from: http://www.ncbi.nlm.nih.gov/pubmed/11826103.

15. Abrahamsson T, Cathala L, Matsui K, Shigemoto R, DiGregorio DA. Thin Dendrites of Cerebellar Interneurons Confer Sublinear Synaptic Integration and a Gradient of Short-Term Plasticity. Neuron. 2012 mar;73(6):1159–1172. Available from: http://linkinghub.elsevier.com/retrieve/pii/S0896627312001821.

16. Cash S, Yuste R. Input summation by cultured pyramidal neurons is linear and position-independent. The Journal of Neuroscience. 1998 jan;18(1):10–15. Available from: http://www.ncbi.nlm.nih.gov/pubmed/9412481.

17. Jia H, Varga Z, Sakmann B, Konnerth A. Linear integration of spine Ca2+ signals in layer 4 cortical neurons in vivo. Proceedings of the National Academy of Sciences of the United States of America. 2014 jun;111(25):9277–82. Available from: http://www.ncbi.nlm.nih.gov/pubmed/24927564.

18. Palmer LM, Shai AS, Reeve JE, Anderson HL, Paulsen O, Larkum ME. NMDA spikes enhance action potential generation during sensory input. Nature Neuroscience. 2014 mar;17(3):383–90. Available from: http://www.ncbi.nlm.nih.gov/pubmed/24487231.

19. Legenstein R, Maass W. Branch-Specific Plasticity Enables Self-Organization of Nonlinear Computation in Single Neurons. Journal of Neuroscience. 2011 jul;31(30):10787–10802. Available from: http://www.jneurosci.org/cgi/doi/10.1523/JNEUROSCI.5684-10.2011.

20. Wu XE, Mel BW. Capacity-enhancing synaptic learning rules in a medial temporal lobe online learning model. Neuron. 2009;62(1):31–41. Available from: http://dx.doi.org/10.1016/j.neuron.2009.02.021http://www.pubmedcentral.nih.gov/articlerender.fcgi?artid=2822782{&}tool=pmcentrez{&}rendertype=abstract.

21. Cazé RD, Foust AJ, Clopath C, Schultz SR. On the distribution and function of synaptic clusters. bioRxiv. 2016;Available from: http://biorxiv.org/content/early/2016/01/31/029330.

22. Häusser M. Synaptic function: Dendritic democracy. Current Biology. 2001;11(1):R10–R12. Available from: http://linkinghub.elsevier.com/retrieve/pii/S0960982200000348.

23. Nevian T, Larkum ME, Polsky A, Schiller J. Properties of basal dendrites of layer 5 pyramidal neurons: a direct patch-clamp recording study. Nature. 2007;200(2):7. Available from: http://www.nature.com/doifinder/10.1038/nn1826http://www.physio.unibe.ch/dendrites/PDFs/Nevian{_}2007{_}NatNeurosci.pdf.

24. Tran-van Minh A, Cazé RD, Abrahamsson T, Cathala L, Gutkin BS, DiGregorio DA. Contribution of sublinear and supralinear dendritic integration to neuronal computations. Frontiers in Cellular Neuroscience. 2015;9(March):1–15.

25. Larkum ME, Waters J, Sakmann B, Helmchen F. Dendritic spikes in apical dendrites of neocortical layer 2/3 pyramidal neurons. The Journal of Neuroscience. 2007 aug;27(34):8999–9008. Available from: http://www.ncbi.nlm.nih.gov/pubmed/17715337.

26. Hill DN, Varga Z, Jia H, Sakmann B, Konnerth A. Multibranch activity in basal and tuft dendrites during firing of layer 5 cortical neurons in vivo. Proceedings of the National Academy of Sciences. 2013;110(33):13618–13623.

27. Cossell L, Iacaruso MF, Muir DR, Houlton R, Sader EN, Ko H, et al. Functional organization of excitatory synaptic strength in primary visual cortex. Nature. 2015;000(00):1–5.

28. Chen TW, Wardill TJ, Sun Y, Pulver SR, Renninger SL, Baohan A, et al. Ultrasensitive fluorescent proteins for imaging neuronal activity. Nature. 2013 jul;499(7458):295–300. Available from: http://www.ncbi.nlm.nih.gov/pubmed/23868258.

29. Go MA, Choy JMC, Colibaba AS, Redman S, Bachor HA, Stricker C, et al. Targeted pruning of a neuron's dendritic tree via femtosecond laser dendrotomy. Scientific Reports. 2016;6(January):19078. Available from: http://www.nature.com/articles/srep19078.

30. Lavzin M, Rapoport S, Polsky A, Garion L, Schiller J. Nonlinear dendritic processing determines angular tuning of barrel cortex neurons in vivo. Nature. 2012 sep;490(7420):397–401. Available from: http://www.nature.com/doifinder/10.1038/nature11451.

31. Lee D, Lin BJ, Lee AK. Hippocampal place fields emerge upon single-cell manipulation of excitability during behavior. Science. 2012 aug;337(6096):849–53. Available from: http://www.ncbi.nlm.nih.gov/pubmed/22904011.

32. Brette R. What Is The Most Realistic Single-Compartment Model of Spike Initiation? 2015;p. 1–13. Available from: http://dx.doi.org/10.1371/journal.pcbi.1004114.

33. Hines ML, Davison AP, Muller E. NEURON and Python. Frontiers in Neuroinformatics. 2009 jan;3(January):1.

34. Bruno RM, Sakmann B. Cortex is driven by weak but synchronously active thalamocortical synapses. Science. 2006 jun;312(5780):1622–7.

35. DeCharms RC, Merzenich MM. Primary cortical representation of sounds by the coordination of action-potential timing. Nature. 1996;381:610–613.